



# Comparative transcriptome analyses of a late-maturing mandarin mutant and its original cultivar reveals gene expression profiling associated with citrus fruit maturation

Lu Wang<sup>1,2</sup>, Qingzhu Hua<sup>1</sup>, Yuewen Ma<sup>1</sup>, Guibing Hu<sup>1</sup> and Yonghua Qin<sup>1</sup>

<sup>1</sup>State Key Laboratory for Conservation and Utilization of Subtropical Agro-bioresources, Key Laboratory of Biology and Genetic Improvement of Horticultural Crops-South China, Ministry of Agriculture, College of Horticulture, South China Agricultural University, Guangzhou, China

<sup>2</sup>Yunnan Key Laboratory for Wild Plant Resources, Key Laboratory for Economic Plants and Biotechnology, Kunming Institute of Botany, Chinese Academy of Sciences, Kunming, China

## ABSTRACT

Characteristics of late maturity in fruit are good agronomic traits for extending the harvest period and marketing time. However, underlying molecular basis of the late-maturing mechanism in fruit is largely unknown. In this study, RNA sequencing (RNA-Seq) technology was used to identify differentially expressed genes (DEGs) related to late-maturing characteristics from a late-maturing mutant ‘Huawan Wuzishatangju’ (HWWZSTJ) (*Citrus reticulata* Blanco) and its original line ‘Wuzishatangju’ (WZSTJ). A total of approximately 17.0 Gb and 84.2 M paired-end reads were obtained. DEGs were significantly enriched in the pathway of photosynthesis, phenylpropanoid biosynthesis, carotenoid biosynthesis, chlorophyll and abscisic acid (ABA) metabolism. Thirteen candidate transcripts related to chlorophyll metabolism, carotenoid biosynthesis and ABA metabolism were analyzed using real-time quantitative PCR (qPCR) at all fruit maturing stages of HWWZSTJ and WZSTJ. Chlorophyllase (*CLH*) and divinyl reductase (*DVR*) from chlorophyll metabolism, phytoene synthase (*PSY*) and capsanthin/capsorubin synthase (*CCS*) from carotenoid biosynthesis, and abscisic acid 8'-hydroxylase (*ABI*) and 9-cis-epoxycarotenoid dioxygenase (*NCED1*) from ABA metabolism were cloned and analyzed. The expression pattern of *NCED1* indicated its role in the late-maturing characteristics of HWWZSTJ. There were 270 consecutive bases missing in HWWZSTJ in comparison with full-length sequences of *NCED1* cDNA from WZSTJ. Those results suggested that *NCED1* might play an important role in the late maturity of HWWZSTJ. This study provides new information on complex process that results in the late maturity of *Citrus* fruit at the transcriptional level.

**Subjects** Agricultural Science, Biotechnology, Molecular Biology, Plant Science

**Keywords** *Citrus reticulata* Blanco, Late maturity, RNA-Seq, Gene expression, *NCED1*

## INTRODUCTION

Fruit maturity date is an important economic trait and selection of varieties with different harvest time would be advantageous to extend their storage period and market share.

Submitted 20 January 2017

Accepted 21 April 2017

Published 18 May 2017

Corresponding author

Yonghua Qin, qinyh@scau.edu.cn

Academic editor

Padmapriya Banada

Additional Information and  
Declarations can be found on  
page 15

DOI 10.7717/peerj.3343

© Copyright  
2017 Wang et al.

Distributed under  
Creative Commons CC-BY 4.0

**OPEN ACCESS**

Citrus, one of the most important fruit crops, is a large-scale commercial production in the tropical and subtropical regions of the world. The total harvested area of citrus exceeds 8.8 million ha, with an annual yield of over 130 million tons in 2015 (*Food and Agricultural Organization of the United Nations, 2014*). Currently, harvest time for most citrus is mainly from November to December resulting in huge market pressure. Therefore, breeding of early- and late-maturing citrus varieties is essential to extend marketing season, meet the needs of consumers and ensure an optimal adaptation to climatic and geographic conditions.

Plant hormones play important roles in the regulation of fruit development and ripening (*Kumar, Khurana & Sharma, 2014*). Ethylene is known to be the major hormonal regulator in climacteric fruit ripening. In addition to ethylene, abscisic acid (ABA), auxin, gibberellin (GA) and brassinosteroid are involved in regulating fruit ripening. ABA plays an important role as an inducer along with ethylene signaling for the onset of fruit degreening and carotenoid biosynthesis during development and ripening process in climacteric and non-climacteric fruits (*Leng et al., 2009; Sun et al., 2010; Jia et al., 2011; Romero, Lafuente & Rodrigo, 2012; Soto et al., 2013; Wang et al., 2016*). ABA treatment can rapidly induce flavonol and anthocyanin accumulation in berry skins of the *Cabernet Sauvignon* grape suggesting that ABA could stimulate berry ripening and ripening-related gene expression (*Koyama, Sadamatsu & Goto-Yamamoto, 2010*). ABA also participates in the regulation of fruit development and ripening of tomato (*Zhang, Yuan & Leng, 2009; Sun et al., 2011*), cucumber (*Wang et al., 2013*), strawberry (*Jia et al., 2011*), bilberry (*Karppinen et al., 2013*), citrus (*Zhang et al., 2014*) and grape (*Nicolas et al., 2014*). Recent studies showed that ABA is a positive regulator of ripening and exogenous ABA application could effectively regulate citrus fruit maturation (*Wang et al., 2016*). Those results suggest that ABA metabolism plays a crucial role in the regulation of fruit development and ripening. In addition, fruit deterioration and post-harvest processes might influence fruit quality and ripening process. However, there are few reports involved in those processes.  $\alpha$ -mannosidase ( $\alpha$ -Man) and  $\beta$ -D-N-acetylhexosaminidase ( $\beta$ -Hex) are the two ripening-specific N-glycan processing enzymes that have proved that their transcripts increased with non-climacteric fruit ripening and softening (*Ghosh et al., 2011*). Genetic results have proved that 9-cis-epoxycarotenoid dioxygenase (NCED) is the key enzyme in ABA metabolism in plants (*Liotenberg, North & Marion-Poll, 1999; Luchi et al., 2001*). *NCED1* could initiate ABA biosynthesis at the beginning of fruit ripening in both peach and grape fruits (*Zhang et al., 2009*). Silence of *FaNCED1* (encoding a key ABA synthesis enzyme) in strawberry fruit could cause the ABA levels to decrease significantly and uncolored fruits and this phenomenon could be rescued by application of exogenous ABA (*Jia et al., 2011*). Suppression of the expression of *SLNCED1* could result in the delay of fruit softening and maturation in tomato (*Sun et al., 2012*). Overexpression of ABA-response element binding factors (*SlAREB1*) in tomato could regulate organic acid and sugar contents during tomato fruit development. Higher levels of organic acid, sugar contents and related-gene expression were detected in *SlAREB1*-overexpressing lines in fruit pericarp of mature tomato (*Bastías et al., 2011*). However, there is little information available about the role of *NCED1* genes in citrus fruit maturation (*Zhang et al., 2014*).

Bud mutant selection is the most common method for creating novel cultivars in *Citrus*. The ‘Huawan Wuzishatangju’ (HWWZSTJ) mandarin is an excellent cultivar derived from a bud sport of a seedless cultivar ‘Wuzishatangju’ (WZSTJ). Fruits of HWWZSTJ are mature in late January to early February of the following year, which is approximately 30 d later than WZSTJ (Qin *et al.*, 2013; Qin *et al.*, 2015). Therefore, the late-maturing mutant and its original cultivar are excellent materials to identify and describe the molecular mechanism involved in citrus fruit maturation. In this study, the highly efficient RNA-Seq technology was used to identify differentially expressed genes (DEGs) between the late-maturing mutant HWWZSTJ and its original line WZSTJ mandarins. DEGs involved in carotenoid biosynthesis, chlorophyll degradation and ABA metabolism were characterized. The present work could help to reveal the molecular mechanism of late-maturing characteristics of citrus fruit at the transcriptional level.

## MATERIALS & METHODS

### Plant materials

The late-maturing mutant ‘Huawan Wuzishatangju’ (HWWZSTJ) (*Citrus reticulata* Blanco) and its original cultivar ‘Wuzishatangju’ (WZSTJ) were planted in the same orchard in South China Agricultural University (23°09′38″N, 113°21′13″E). Ten six-year-old trees of each cultivar were used in this experiment. Peels (including albedo and flavedo fractions) from fifteen uniform-sized fresh fruits were collected on the 275<sup>th</sup> (color-break stage, i.e., peels turns from green to orange) and 320<sup>th</sup> (maturing stage) days after flowering (DAF) of HWWZSTJ and 275<sup>th</sup> (maturing stage) DAF of WZSTJ (Fig. S1) in 2012 and pools were named T3, T1 and T2, respectively. Peels from fifteen uniform-sized fresh fruits of HWWZSTJ and WZSTJ were collected on the 255<sup>th</sup>, 265<sup>th</sup>, 275<sup>th</sup>, 285<sup>th</sup>, 295<sup>th</sup>, 305<sup>th</sup>, 315<sup>th</sup> and 320<sup>th</sup> DAF in 2012 and used for expression analyses of candidate transcripts associated with chlorophyll, carotenoid biosynthesis and ABA metabolism. All samples were immediately frozen in liquid nitrogen and stored at −80 °C until use.

### RNA extraction, library construction and RNA-Seq

Total RNA was extracted from peels according to the protocol of the RNAout kit (Tiandz, Beijing, China) and genomic DNA was removed by DNase I (TaKaRa, Dalian, China). RNA quality was analyzed by 1.0% agarose gel and its concentration was quantified by a NanoDrop ND1000 spectrophotometer (NanoDrop Technologies, Wilmington, DE, USA). RNA integrity number (RIN) values (>7.0) were assessed using an Agilent 2100 Bioanalyzer (Agilent Technologies, Santa Clara, CA, USA).

Construction of RNA-Seq libraries was performed by the Biomarker Biotechnology Corporation (Beijing, China). mRNA was enriched and purified with oligo (dT)-rich magnetic beads and then broken into short fragments. The cleaved RNA fragments were reversely transcribed to the first-strand cDNA using random hexamer primers. The second-strand cDNA was synthesized using RNase H and DNA polymerase I. The cDNA fragments were purified, end blunted, ‘A’ tailed, and adaptor ligated. The distribution sizes of the cDNA in the three libraries were monitored using an Agilent 2100 bioanalyzer. Finally, the three libraries were sequenced using an Illumina HiSeq™ 2500 platform.

## Transcriptome assembly and annotation

Sequences obtained in this study were annotated in reference to the genome sequence of *Citrus sinensis* (Xu et al., 2013; Wang et al., 2014) using a TopHat program (Trapnell, Pachter & Salzberg, 2009). Functional annotation of the unigenes was performed using BLASTx (Altschul et al., 1997) and classified by Swiss-Prot (SWISS-PROT downloaded from European Bioinformatics Institute by Jan., 2013), Clusters of Orthologous Groups of Proteins Database (COG) (Tatusov et al., 2000), Kyoto Encyclopedia of Genes and Genomes Database (KEGG, release 58) (Kanehisa et al., 2004), non-redundant (nr) (Deng et al., 2006) and Gene Ontology (GO) (Harris et al., 2004). The number of mapped and filtered reads for each unigene was calculated and normalized giving the corresponding Reads Per Kilobases per Million reads (RPKM) values. DEGs between the two samples were determined according to a false discovery rate (FDR) threshold of <0.01, an absolute log<sub>2</sub> fold change value of  $\geq 1$  and a *P*-value <0.01.

## Gene validation and expression analysis

Data from RNA-Seq were validated using qPCR. All pigment-related (chlorophyll metabolism, carotenoid biosynthesis and ABA metabolism) uni-transcripts were selected to elucidate their expression patterns at all peel coloration stages of HWWZSTJ and WZSTJ with specific primers (Table S1). The citrus *actin* gene (accession No. GU911361.1) was used as an internal standard for the normalization of gene expression. Expression levels of all pigment-related uni-transcripts were determined using qPCR in an Applied Biosystems 7500 real-time PCR system (Applied Biosystems, CA, USA). A total of 20.0  $\mu$ l reaction volume contained 10.0  $\mu$ l THUNDERBIRD SYBR qPCR Mix (TOYOBO Co., Ltd.), 50 $\times$ ROX Reference dye, 2.0  $\mu$ l Primer Mix (5.0  $\mu$ M), 6.0  $\mu$ l ddH<sub>2</sub>O, and 2.0  $\mu$ l cDNA (40 ng). The qPCR parameters were: 94 °C for 60 s then 40 cycles of 95 °C for 15 s, 55 °C for 15 s and 72 °C for 30 s. All experiments were performed three times with three biological replicates. Relative expression levels of selected transcripts were calculated by the  $2^{-\Delta\Delta CT}$  method (Livak & Schmittgen, 2011).

All pigment-related genes (chlorophyll metabolism, carotenoid biosynthesis, ABA metabolism) were cloned using specific primers (Table S2). The 20.0  $\mu$ l of reaction volume contained 2.0  $\mu$ l 10 $\times$ PCR buffer, 2.0  $\mu$ l dNTP (2.0 mM), 0.2  $\mu$ l of each primer (10  $\mu$ M), 2.0  $\mu$ l DNA (100 ng), 0.2  $\mu$ l LA *Taq* and 13.4  $\mu$ l ddH<sub>2</sub>O. PCR reaction procedure was 94 °C for 4 min then 35 cycles of 94 °C for 30 s, 55 °C for 30 s and 72 °C for 2 min, with a final 72 °C for 10 min. Nucleotide sequences of the pigment-related genes were analyzed using the National Center for Biotechnology Information (NCBI) Blast program (<http://www.ncbi.nlm.nih.gov/BLAST>). ORFs were made using the NCBI ORF Finder (<http://www.ncbi.nlm.nih.gov/gorf/gorf.html>). Alignments were done using ClustalX 1.83 and DNAMAN software. Phylogenetic analysis of deduced amino acid sequences were performed using MEGA (version 5.0) and the Neighborjoining method with 1,000 bootstrap replicates.

**Table 1** Summary of the sequencing data.

Samples	Total reads	Total base	GC content (%)	Q30 (%)
T1	26,403,257	5,332,498,617	44.27	94.11
T2	29,163,126	5,890,197,025	44.62	93.98
T3	28,606,868	5,777,864,876	44.20	93.90

**Notes.**

T1, HWWZSTJ (320 DAF); T2, WZSTJ (275 DAF); T3, HWWZSTJ (275 DAF).

**Table 2** Summary of the transcriptome annotation compared with the reference genome of *C. Sinensis* (Xu et al., 2013).

Statistics libraries	T1		T2		T3	
	Number	Percentage	Number	Percentage	Number	Percentage
Total reads	52,806,514	100.0%	58,326,252	100.0%	57,213,736	100.0%
Mapped reads	44,664,047	84.58%	49,507,338	84.88%	48,492,905	84.76%
Unique mapped reads	43,386,022	97.14%	48,146,871	97.25%	47,129,445	97.19%
Multiple mapped reads	1,278,025	2.86%	1,360,467	2.75%	1,363,460	2.81%
Pair mapped reads	39,251,294	87.88%	43,459,426	87.78%	42,663,447	87.98%
Single mapped reads	4,574,673	10.24%	5,159,966	10.42%	4,969,429	10.25%

**Notes.**

T1, HWWZSTJ (320 DAF); T2, WZSTJ (275 DAF); T3, HWWZSTJ (275 DAF).

## RESULTS

### RNA-Seq analyses

To obtain differentially expressed genes (DEGs) between HWWZSTJ and WZSTJ, three libraries (T1, T2 and T3) were designed for RNA-Seq. As shown in Table 1, 26,403,257, 29,163,126, and 28,606,868 raw reads were obtained respectively from the three libraries. After removing low-quality bases and reads, a total of approximately 17.0 Gb clean reads were obtained. The GC contents for T1, T2 and T3 were 44.27%, 44.62% and 44.20%, respectively (Table 1). The range of most transcripts length was 100–200 bp (Fig. S2). Q30 percentage (percentage of sequences with sequencing error rate lower than 0.01%) for each sample was over 90% (Table 1).

A total of 44,664,047, 49,507,338 and 48,492,905 reads were mapped which accounted for 84.58%, 84.88% and 84.76% of the total reads, respectively (Table 2). Number of unique mapped reads accounted for 97.14% (T1), 97.25% (T2) and 97.19% (T3) of the total mapped reads compared with 2.86% (T1), 2.75% (T2) and 2.81% (T3) for multiple mapped reads, respectively. Those results suggested that the throughput and sequencing quality was high enough for further analyses.

### Analyses of differentially expressed genes (DEGs)

DEGs were screened by comparison between any two of the three libraries using  $p < 0.01$ ,  $FDR < 0.01$  and  $Fold\ Change \geq 2$  as thresholds. A total of 2,687, 3,002 and 1,834 DEGs were obtained between the T1 and T3, T2 and T1, T2 and T3 libraries, respectively (Fig. 1A). Among those DEGs, 1,162, 1,567 and 770 were up-regulated and 1,525, 1,435 and 1,064 were down-regulated (Fig. 1B). Transcriptional levels of DEGs in HWWZSTJ on

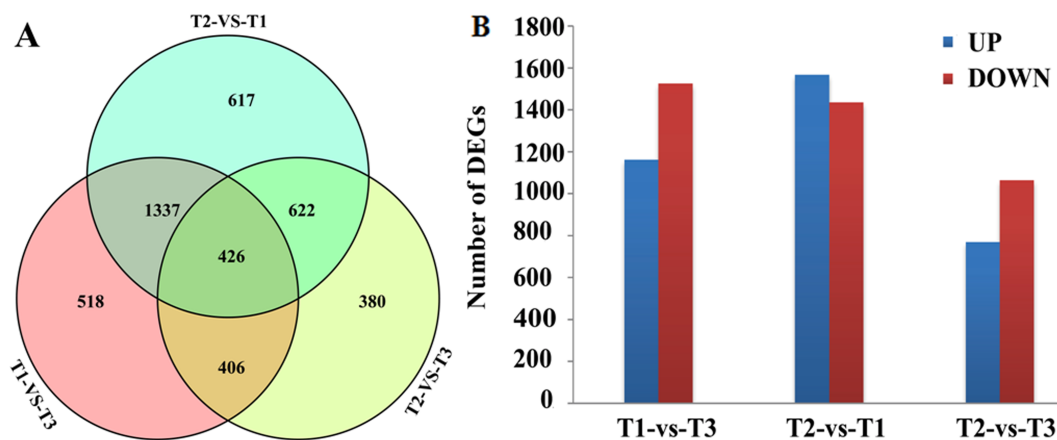


**Figure 1** Venn diagram (A) and histogram (B) of DEGs. T1, HWWZSTJ (320 DAF); T2, WZSTJ (275DAF); T3, HWWZSTJ (275DAF).

320<sup>th</sup> DAF were lower than that on 275<sup>th</sup> DAF in HWWZSTJ suggesting that transcriptional levels of DEGs decreased during fruit maturation in HWWZSTJ (Fig. 1B).

### Functional annotation of transcripts

A total of 299 new transcripts were annotated using five public databases (Nr, Swiss-Prot, KEGG, COG and GO). A summary of the annotations was shown in Table S3. Maximum number of annotation of differentially expressed transcripts (2,954) was in the Nr databases by comparison between T1 and T3, T2 and T1, T2 and T3, followed by GO databases (2,648) (Table S4). The differentially expressed transcripts were classified into three categories in GO assignments: cellular component, molecular function and biological process. DEGs between T1 and T3, T2 and T1, T2 and T3 were all significantly enriched in pigmentation, signaling and growth biological processes (Fig. S3A). Based on COG classifications, differentially expressed transcripts were divided into 25 different functional groups (Fig. S3B). DEGs between any two of the three libraries (T1-VS-T3, T2-VS-T1, T2-VS-T3) were assigned to 91, 100 and 91 KEGG pathways, respectively (File S1), and phenylalanine metabolism, porphyrin and chlorophyll metabolism, and flavonoid biosynthesis were the three significantly enriched biological processes (Table 3).

### Verification of the accuracy of the RNA-Seq data using qPCR

Twelve DEGs with significant differences from the three libraries were selected for verification of RNA-Seq data by qPCR. Linear regression analysis showed an overall correlation coefficient of 0.828, indicating a good correlation between qPCR results and the transcripts per kilobase million from the RNA-Seq data (Fig. S4).

### DEGs related to carotenoid biosynthesis, chlorophyll and ABA metabolism

Analyses of the expression data obtained through RNA-Seq revealed that most DEGs were involved in carotenoid biosynthesis, chlorophyll and ABA metabolism. The main transcripts involved in the three pathways were shown in Table 4 and heatmaps were made

**Table 3** Analyses of differentially expressed transcripts based on KEGG pathway.

#	Pathway	DEGs with pathway annotation (283)	All genes with pathway annotation (3516)	p_value	corr_p_value	Pathway ID
T1 vs T3	1 Phenylpropanoid biosynthesis	24 (8.48%)	82 (2.33%)	9.58e−09	8.71e−07	ko00940
	2 Photosynthesis	14 (4.95%)	46 (1.31%)	7.90e−06	7.19e−04	ko00195
	3 Plant-pathogen interaction	26 (9.19%)	130 (3.7%)	8.30e−06	7.56e−04	ko04626
	4 Plant hormone signal transduction	31 (10.95%)	180 (5.12%)	2.73e−05	2.49e−03	ko04075
	5 Phenylalanine metabolism	17 (6.01%)	72 (2.05%)	3.59e−05	3.26e−03	ko00360
	6 Photosynthesis-antenna proteins	7 (2.47%)	15 (0.43%)	7.45e−05	6.78e−03	ko00196
	7 Galactose metabolism	10 (3.53%)	45 (1.28%)	2.46e−03	2.23e−01	ko00052
	8 Starch and sucrose metabolism	21 (7.42%)	137 (3.9%)	2.66e−03	2.42e−01	ko00500
	9 Porphyrin and chlorophyll metabolism	8 (2.83%)	37 (1.05%)	7.83e−03	7.12e−01	ko00860
	10 Amino sugar and nucleotide sugar metabolism	14 (4.95%)	89 (2.53%)	1.06e−02	9.66e−01	ko00520
T2 vs T1	1 Photosynthesis	18 (5.17%)	46 (1.31%)	1.1384e−07	1.1384e−05	ko00195
	2 Photosynthesis antenna proteins	10 (2.87%)	15 (0.43%)	1.5234e−07	1.5234e−05	ko00196
	3 Plant-pathogen interaction	32 (9.2%)	130 (3.7%)	5.5471e−07	5.5471e−05	ko04626
	4 Phenylpropanoid biosynthesis	22 (6.32%)	82 (2.33%)	7.9820e−06	7.9820e−04	ko00940
	5 Cyanoamino acid metabolism	9 (2.59%)	22 (0.63%)	1.2713e−04	1.2713e−02	ko00460
	6 Biosynthesis of unsaturated fatty acids	9 (2.59%)	29 (0.82%)	1.3656e−03	1.3656e−01	ko01040
	7 Phenylalanine metabolism	16 (4.6%)	72 (2.05%)	1.3850e−03	1.3850e−01	ko00360
	8 Flavonoid biosynthesis	10 (2.87%)	37 (1.05%)	2.3996e−03	2.3996e−01	ko00941
	9 Starch and sucrose metabolism	23 (6.61%)	137 (3.9%)	7.1760e−03	7.1760e−01	ko00500
	10 Stilbenoid, diarylheptanoid and gingerol biosynthesis	5 (1.44%)	14 (0.4%)	8.6944e−03	8.6944e−01	ko00945
T2 vs T3	1 Photosynthesis	26 (10.48%)	46 (1.31%)	5.1027e−19	4.6434e−17	ko00195
	2 Photosynthesis-antenna proteins	11 (4.44%)	15 (0.43%)	1.8431e−10	1.6772e−08	ko00196
	3 Phenylpropanoid biosynthesis	24 (9.68%)	82 (2.33%)	6.3286e−10	5.7590e−08	ko00940
	4 Phenylalanine metabolism	16 (6.45%)	72 (2.05%)	2.6448e−05	2.4068e−03	ko00360
	5 Nitrogen metabolism	9 (3.63%)	32 (0.91%)	2.4845e−04	2.2609e−02	ko00910
	6 Flavone and flavonol biosynthesis	6 (2.42%)	15 (0.43%)	3.3744e−04	3.0707e−02	ko00944
	7 Cyanoamino acid metabolism	7 (2.82%)	22 (0.63%)	5.4299e−04	4.9412e−02	ko00460
	8 Stilbenoid, diarylheptanoid and gingerol biosynthesis	5 (2.02%)	14 (0.4%)	1.9788e−03	1.8007e−01	ko00945
	9 Glyoxylate and dicarboxylate metabolism	7 (2.82%)	28 (0.8%)	2.6144e−03	2.3791e−01	ko00630
	10 Flavonoid biosynthesis	8 (3.23%)	37 (1.05%)	3.5075e−03	3.1918e−01	ko00941
	11 Porphyrin and chlorophyll metabolism	8 (3.23%)	37 (1.05%)	3.5075e−03	3.1918e−01	ko00860
	12 Plant-pathogen interaction	18 (7.26%)	130 (3.7%)	3.9071e−03	3.5554e−01	ko04626

based on transcripts per kilobase million from the RNA-Seq data (Fig. 2). Three transcripts (*Cs8g15480*, Pheophorbide a oxygenase; *Cs5g16830*, Chlorophyllase type 0 and *Cs3g19690*, Chlorophyll synthase) involved in chlorophyll degradation, six transcripts (*Cs3g19770*, Delta-aminolevulinic acid dehydratase; *Cs9g13460*, Magnesium-chelatase subunit H; *Cs2g05100*, Magnesium-chelatase subunit ChII-1; *Cs7g19710*, Magnesium-protoporphyrin O-methyltransferase; *Cs6g16200*, Magnesium-protoporphyrin IX monomethyl ester

**Table 4** Analyses of transcripts involved in carotenoid biosynthesis, chlorophyll and ABA metabolism.

Gene ID	RPKM			Nr-annotation
	T1	T2	T3	
<b>Chlorophyll metabolism</b>				
<i>Cs3g03100</i>	69.88	63.55	72.16	Probable glutamate-tRNA ligase [ <i>Arabidopsis thaliana</i> ]
<i>Cs8g01360</i>	56.22	59.50	59.42	Glutamate-tRNA ligase 1 [ <i>Arabidopsis thaliana</i> ]
<i>Cs3g16730</i>	78.03	66.88	70.76	Glutamyl-tRNA reductase 1 [ <i>Arabidopsis thaliana</i> ]
<i>Orange1.1t02623</i>	89.64	138.40	164.18	Glutamate-1-semialdehyde 2,1-aminomutase 1, Chloroplastic [ <i>Arabidopsis thaliana</i> ]
<i>Cs3g19770</i>	35.03	42.97	62.68	Delta-aminolevulinic acid dehydratase, chloroplastic [ <i>Arabidopsis thaliana</i> ]
<i>Cs7g13850</i>	16.13	23.66	30.83	Porphobilinogen deaminase [ <i>Arabidopsis thaliana</i> ]
<i>Cs5g12440</i>	21.59	19.34	27.86	Uroporphyrinogen decarboxylase 1, chloroplastic
<i>Cs7g30080</i>	53.66	58.13	83.90	Uroporphyrinogen decarboxylase 2, chloroplastic
<i>Orange1.1t02279</i>	37.48	71.77	87.12	Coproporphyrinogen-III oxidase, chloroplastic
<i>Cs5g06770</i>	4.31	6.90	7.22	Oxygen-independent coproporphyrinogen-III oxidase 1
<i>Cs2g24910</i>	21.98	25.25	31.77	Protoporphyrinogen oxidase, chloroplastic/mitochondrial
<i>Orange1.1t01782</i>	35.37	56.42	53.75	Protoporphyrinogen oxidase, chloroplastic
<i>Cs9g13460</i>	44.52	5.36	17.65	Magnesium-chelatase subunit H
<i>Cs2g30990</i>	16.52	19.32	21.84	Magnesium-chelatase 67 kDa subunit
<i>Cs2g05100</i>	118.46	82.35	183.85	Magnesium-chelatase subunit ChII-1, chloroplastic
<i>Cs7g19710</i>	6.74	3.42	18.65	Magnesium-protoporphyrin O-methyltransferase
<i>Cs6g16200</i>	76.55	14.23	116.31	Magnesium-protoporphyrin IX monomethyl ester [oxidative] cyclase 1
<i>Cs1g06850</i>	22.97	15.00	167.60	Protochlorophyllide reductase A, chloroplastic
<i>Cs5g16830</i>	5.28	29.95	0.81	Chlorophyllase type 0
<i>Cs9g07520</i>	30.05	13.07	20.43	Chlorophyllase type 0
<i>Cs6g08720</i>	57.16	45.38	61.05	Bacteriochlorophyll synthase 34 kDa chain
<i>Cs3g19690</i>	47.34	3.63	10.36	Chlorophyll synthase, putative [ <i>Ricinus communis</i> ]
<i>Cs4g15890</i>	56.44	69.89	61.91	Chlorophyll (ide) b reductase NOL, chloroplastic
<i>Cs7g24010</i>	5.24	11.18	13.54	Chlorophyll (ide) b reductase NOL, chloroplastic
<i>Cs8g15480</i>	64.04	92.78	73.45	Pheophorbide a oxygenase, chloroplastic
<i>Cs1g22670</i>	37.78	73.56	82.11	Red chlorophyll catabolite reductase, chloroplastic
<b>Carotenoid biosynthesis</b>				
<i>Cs6g15910</i>	79.73	216.13	172.64	Phytoene synthase
<i>Orange1.1t02108</i>	30.15	85.62	32.83	PREDICTED: phytoene synthase 2, chloroplastic-like [ <i>Vitis vinifera</i> ]
<i>Orange1.1t02361</i>	50.61	63.09	64.41	Phytoene dehydrogenase, chloroplastic/chromoplastic
<i>Cs5g24730</i>	47.11	59.11	58.21	15-cis-zeta-carotene isomerase, chloroplastic
<i>Cs3g11180</i>	56.36	81.36	70.96	Phytoene dehydrogenase, chloroplastic/chromoplastic
<i>Cs6g13340</i>	25.39	26.28	23.76	Prolycopene isomerase 1, chloroplastic
<i>Cs4g14850</i>	7.43	5.56	10.07	Capsanthin/capsorubin synthase, chromoplast
<i>Orange1.1t00772</i>	9.33	8.65	11.12	Capsanthin/capsorubin synthase, chromoplast

(continued on next page)



Table 4 (continued)

Gene ID	RPKM			Nr-annotation
	T1	T2	T3	
<i>Orange1.1t01058</i>	38.85	39.93	39.95	Cytochrome P450 97B1, chloroplastic
<i>Cs9g19270</i>	1038.75	1722.54	1359.83	Beta-carotene 3-hydroxylase 1, chloroplastic
<i>Cs1g22620</i>	65.41	82.35	95.98	3-hydroxybenzoate 6-hydroxylase 1
<i>Orange1.1t04051</i>	1.01	0.95	1.10	3-hydroxybenzoate 6-hydroxylase 1
<i>Cs5g26080</i>	11.76	9.88	16.31	Violaxanthin de-epoxidase, chloroplastic
<i>Orange_new Gene_1755</i>	0.45	3.82	9.60	Lycopene beta-cyclase [ <i>Citrus × paradisi</i> ]
<b>ABA metabolism</b>				
<i>Cs8g13780</i>	4.47	3.20	4.51	Indole-3-acetaldehyde oxidase
<i>Cs6g01180</i>	46.39	38.09	60.42	Xanthoxin dehydrogenase
<i>Cs2g03270</i>	2.08	67.84	18.90	9-cis-epoxycarotenoid dioxygenase 2 [ <i>Citrus sinensis</i> ]
<i>Cs5g14370</i>	28.65	20.09	8.45	Putative 9-cis-epoxycarotenoid dioxygenase 3 [ <i>Citrus sinensis</i> ]
<i>Cs7g14820</i>	2.18	0.26	5.90	Carotenoid cleavage dioxygenase 4a [ <i>Citrus clementina</i> ]
<i>Cs9g11260</i>	0.00	0.00	0.00	Carotenoid 9,10(9,10')-cleavage dioxygenase 1
<i>Cs6g19380</i>	60.57	30.48	9.86	ABA 8&apos; -hydroxylase [ <i>Citrus sinensis</i> ]
<i>Cs8g05940</i>	2.05	3.80	3.20	Abscisic acid 8'-hydroxylase 1
<i>Cs8g18780</i>	1.10	0.78	0.27	ABA 8&apos; -hydroxylase [ <i>Citrus sinensis</i> ]

(oxidative) cyclase 1 and *Cs1g06850*, Protochlorophyllide reductase A) involved in chlorophyll biosynthesis, five transcripts (*Cs6g15910*, Phytoene synthase; *Orange1.1t02108*, phytoene synthase 2; *Cs6g13340*, Prolycopene isomerase 1; *Cs4g14850/Orange1.1t00772*, Capsanthin/capsorubin synthase and *Orange\_new Gene\_1755*, Lycopene beta-cyclase) involved in carotenoid biosynthesis and four transcripts (*Cs2g03270/Cs5g14370*, 9-cis-epoxycarotenoid dioxygenase 2; *Cs6g01180*, Xanthoxin dehydrogenase; *Cs7g14820*, Carotenoid cleavage dioxygenase 4a and *Cs6g19380*, ABA 8&apos; -hydroxylase) involved in ABA metabolism were obtained (Fig. 2 and Table 4).

According to the result of expression and annotation analyses, thirteen transcripts i.e., *BCHP*, *CRD1*, *CHLM*, *CHLH1*, *HEMFI/HEMF2*, *FC1*, *DVR*, *CAO*, *CLH*, *CCS*, *PSY*, *AB* and *NCED1* associated with chlorophyll metabolism, carotenoid biosynthesis and ABA metabolism were obtained with a Fold Change  $\geq 2$  and FDR  $< 0.01$  as screening standard (Table 5).

### Expression analyses of candidate transcripts

Expression patterns of candidate transcripts associated with chlorophyll metabolism were analyzed between WZSTJ and HWWZSTJ at all fruit maturation stages (Fig. 3). Compared with WZSTJ, lower expression levels of *ALAD1* and *CLH* were detected in HWWZSTJ at all fruit maturation stages. Expression of *ALAD1* and *CLH* were increasing before fruit maturation and decreased thereafter in both WZSTJ and HWWZSTJ. The highest expression level of *CLH* was detected on the 295<sup>th</sup> DAF in HWWZSTJ, which was 20 d later than WZSTJ. Expression levels of *CAO1* and *PAO* in HWWZSTJ was higher than that in WZSTJ. *FC1* showed a decrease trend during fruit maturation of WZSTJ and HWWZSTJ.

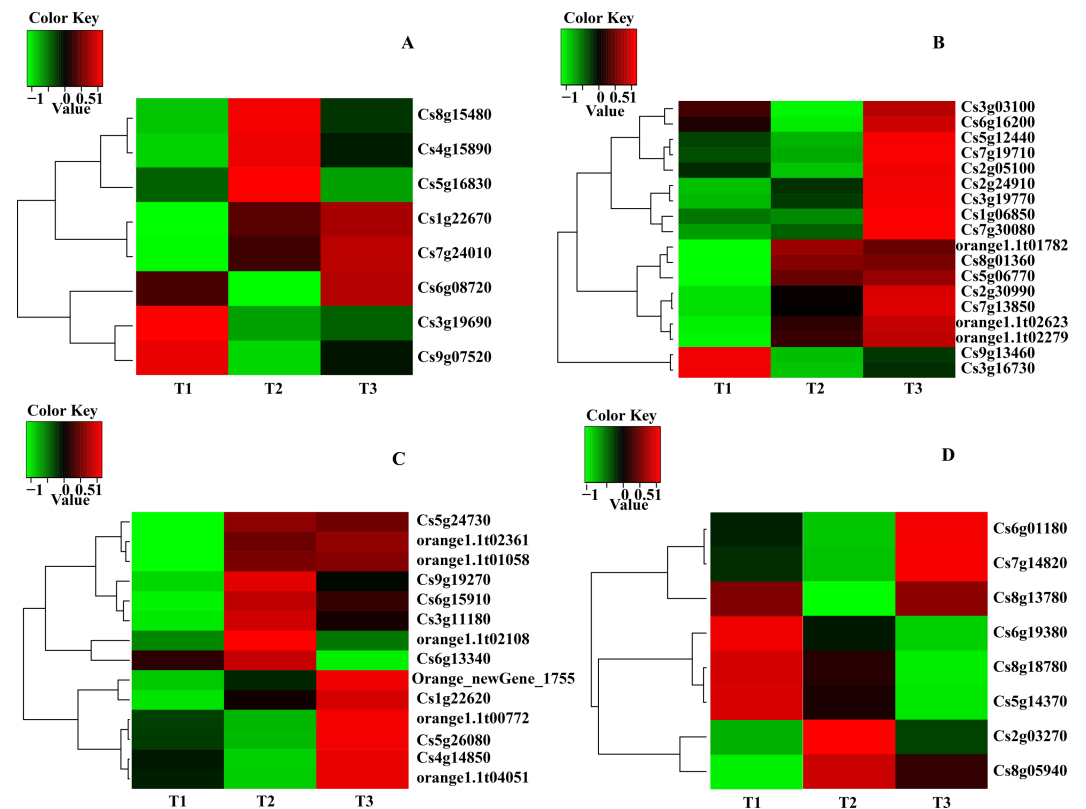


**Figure 2** Heatmap of main transcripts from chlorophyll metabolism (A), chlorophyll synthesis (B), carotenoid biosynthesis (D) and ABA metabolism (C).

As for *GluRS*, *HEMF1*, *HEMG* and *CHLM*, they showed irregular expression patterns in WZSTJ and HWWZSTJ (Fig. 3).

Six carotenoid biosynthesis-related transcripts showed a trend from rise to decline at all fruit maturation stages of WZSTJ and HWWZSTJ (Fig. 4). The highest expression level of *CCS* was detected on the 295<sup>th</sup> DAF in HWWZSTJ, which was 20 d later than that of WZSTJ. Expression levels of *PDS1*, *PSY3*, *PSY5*, *PSY6* and *PSY7* in WZSTJ were higher than that of HWWZSTJ. *PDS1* showed an increasing trend during fruit maturation of WZSTJ and HWWZSTJ and reached its maximum expression on the 295<sup>th</sup> DAF. *PSY5* showed the highest expression levels on the 275<sup>th</sup> DAF compared to the highest expression levels of *PSY3*, *PSY6* and *PSY7* on the 265<sup>th</sup> DAF in both WZSTJ and HWWZSTJ. Expression levels of *PSY5* were increasing before the 275<sup>th</sup> DAF and decreased thereafter. *PSY3*, *PSY6* and *PSY7* were up-regulation before the 265<sup>th</sup> DAF and decreased gradually thereafter (Fig. 4).

Expression patterns of two candidate transcripts i.e., *ABI* and *NCED1* related to ABA metabolism were analyzed at all fruit maturation stages of WZSTJ and HWWZSTJ (Fig. 5). *ABI* showed a trend from rise to decline during fruit maturation stages of WZSTJ and HWWZSTJ. The highest expression level of *ABI* was obtained on the 295<sup>th</sup> DAF in HWWZSTJ, which was 20 d later than WZSTJ. Similar expression patterns of *NCED1* were observed before the 295<sup>th</sup> DAF in HWWZSTJ and WZSTJ (Fig. 5). The expression level

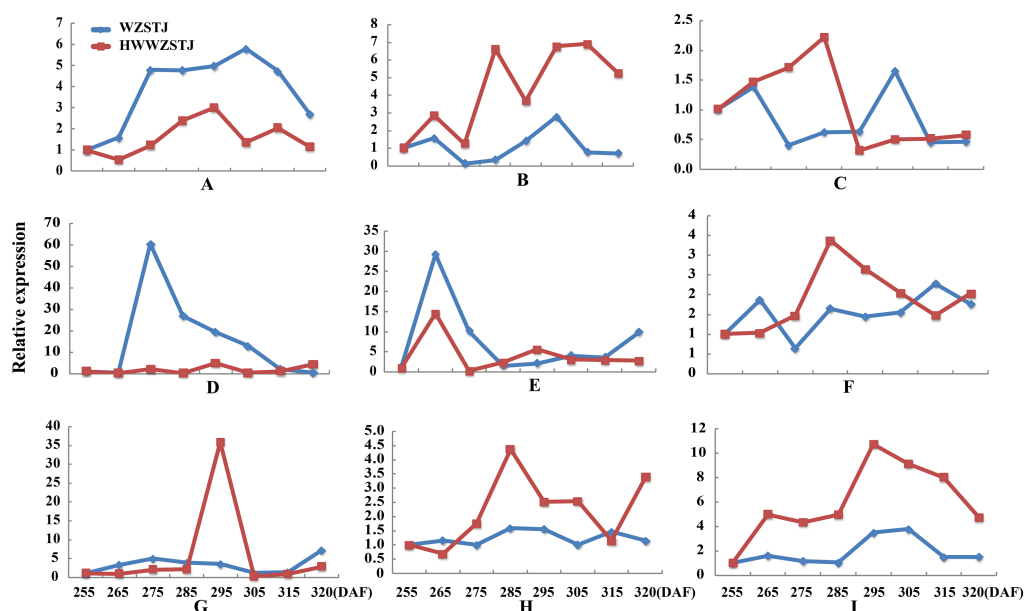


**Figure 3** Expression patterns of genes associated with chlorophyll metabolism in WZSTJ and HWWZSTJ at all fruit maturation stages. (A) *ALAD1*; (B) *CAO1*; (C) *CHLM*; (D) *CLH*; (E) *FCI*; (F) *GluRs*; (G) *HEMF1*; (H) *HEMG*; (I) *PAO*.

**Table 5** Analyses of DEGs associated with carotenoid biosynthesis, chlorophyll and ABA metabolism.

Gene ID	Symbols
<b>Chlorophyll metabolism</b>	
<i>Cs5g10740/ Cs2g26780</i>	Geranyl acyl geranyl acyl diphosphate reductase ( <i>BCHP</i> )
<i>Cs6g16200</i>	Methyl magnesium protoporphyrin IX single cyclase ( <i>CRD1</i> )
<i>Cs7g19710</i>	Magnesium protoporphyrin IX methyl transferase ( <i>CHLM</i> )
<i>Cs2g05100/ Cs9g13460</i>	Mg-chelatase subunit D ( <i>CHLD</i> )/Mg-chelatase subunit H ( <i>CHLH1</i> )
<i>Orange1.1t02279</i>	Coproporphyrin oxidative decarboxylase ( <i>HEMF1/HEMF2</i> )
<i>Cs4g18730</i>	Ferrochelatase ( <i>FCI</i> )
<i>Cs1g06850</i>	Divinyl reductase ( <i>DVR</i> )
<i>Cs3g19690</i>	Chlorophyllide a oxygenase ( <i>CAO</i> )
<i>Cs5g16830</i>	Chlorophyllase ( <i>CLH</i> )
<b>Carotenoid biosynthesis</b>	
<i>Orange_new Gene_1755</i>	Capsanthin/capsorubin synthase ( <i>CCS</i> )
<i>Orange1.1t02108/Cs6g15910</i>	Phytoene synthase ( <i>PSY</i> )
<b>ABA metabolism</b>	
<i>Cs3g23530</i>	Abscisic acid 8'-hydroxylase ( <i>AB</i> )
<i>Cs5g14370</i>	9-cis-epoxycarotenoid dioxygenase ( <i>NCED1</i> )

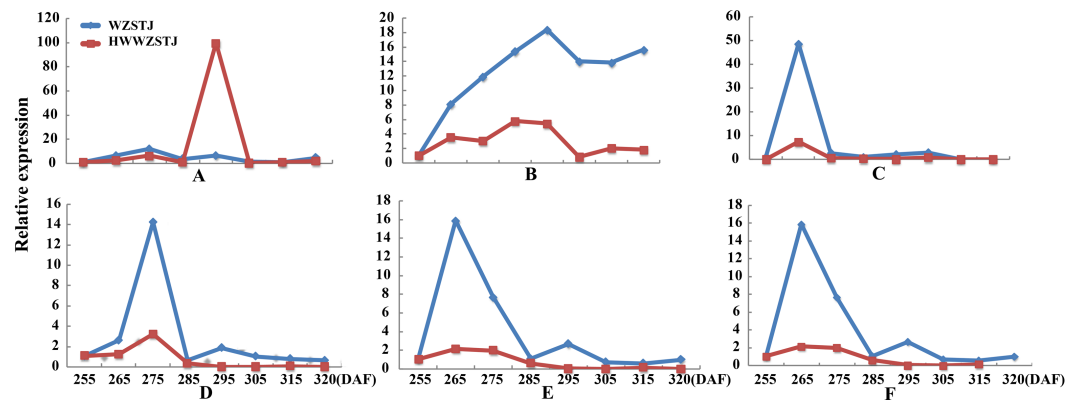


**Figure 4** Expression patterns of genes associated with carotenoid biosynthesis in WZSTJ and HWWZSTJ at all fruit maturation stages. (A) *CCS*; (B) *PDS1*; (C) *PSY3*; (D) *PSY5*; (E) *PSY6*; (F) *PSY7*.

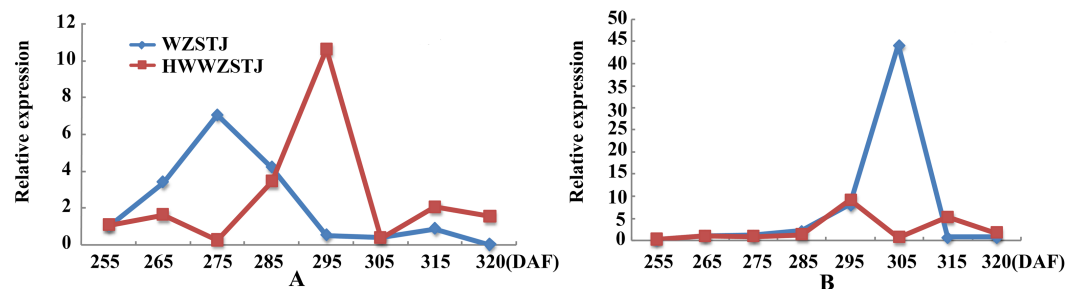


**Figure 5** Expression patterns of transcripts associated with ABA metabolism in WZSTJ and HWWZSTJ at all fruit maturation stages. (A) *ABI1*; (B) *NCED1*.

of *NCED1* in HWWZSTJ was lower than that of WZSTJ during 275<sup>th</sup> DAF to 305<sup>th</sup> DAF. The highest expression level of *NCED1* was detected on the 305<sup>th</sup> DAF of WZSTJ and significantly decreased thereafter (Fig. 5). However, the highest expression of *NCED1* was at 295 DAF in HWWZSTJ. Results from expression analyses of candidate genes suggested that *NCED1* might play a leading role in late-maturing characteristics of HWWZSTJ.

### Cloning and phylogenetic analyses of candidate genes

Full-length cDNA sequences of *CLH* and *DVR* from chlorophyll metabolism, *PSY3*, *PSY5*, *PSY6*, *PSY7* and *CCS* from carotenoid biosynthesis, *ABI1* and *NCED1* from ABA metabolism were cloned from HWWZSTJ and WZSTJ mandarins. There was one difference in base pair of *CLH*, *PSY3* and *PSY5* cDNA sequences between HWWZSTJ and WZSTJ (Figs. S5–S7). However, the amino acid sequences of *CLH*, *PSY3* and *PSY5* from HWWZSTJ was 100% identical to that from WZSTJ. There were 4, 6, 4, 3 and 17 bp difference between the sequences of *DVR*, *CCS*, *PSY6*, *PSY7* and *ABI1* derived from HWWZSTJ and WZSTJ and this resulted in 2, 3, 3, 1 and 8 differences in the amino acids that would have been incorporated during translation of these transcripts (Figs. S8–S12). Compared with WZSTJ,

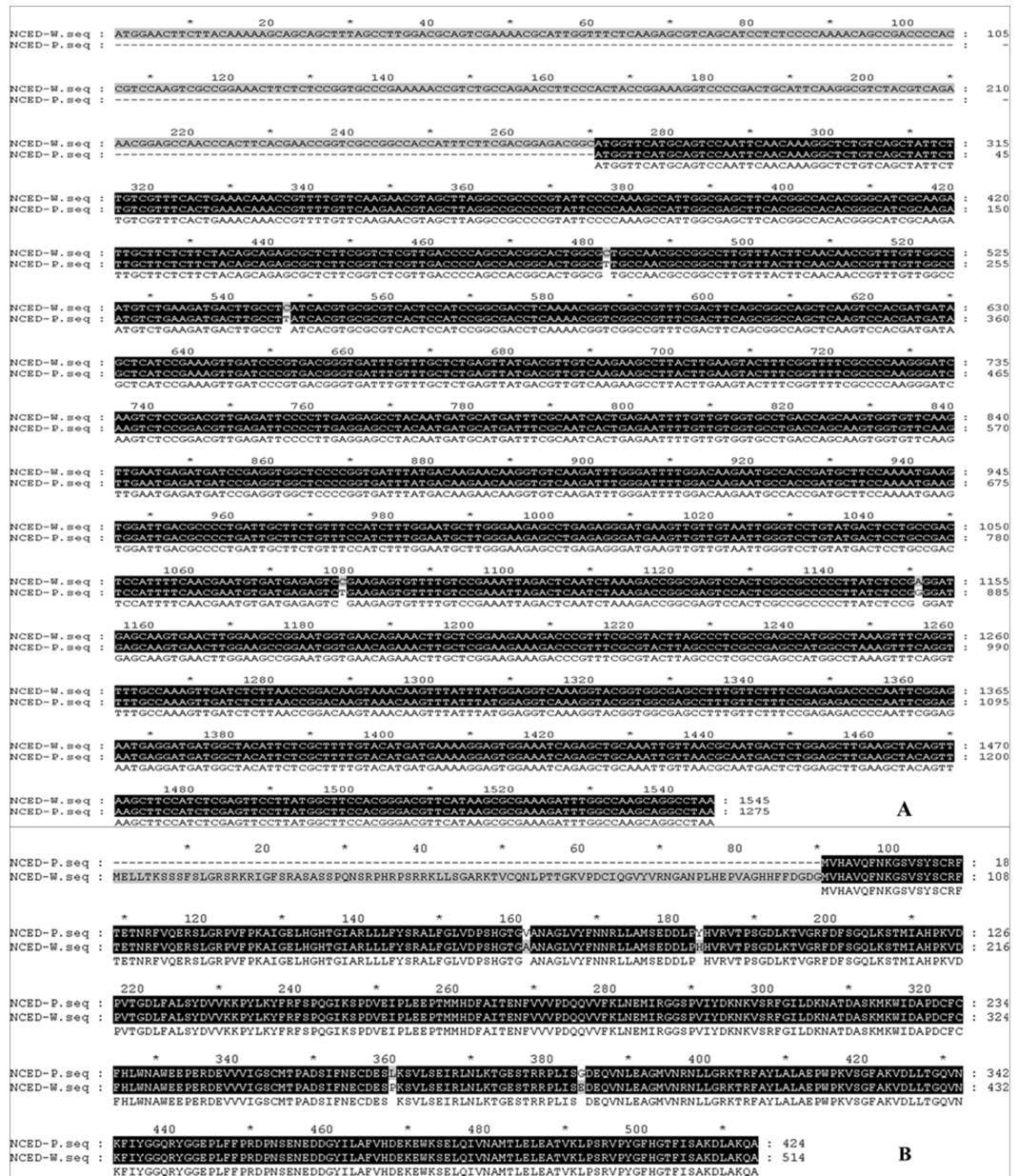


**Figure 6** Alignments of cDNA (A) and amino acid (B) sequences of the *NCED1* from HWWZSTJ and WZSTJ. W, HWWZSTJ; P, WZSTJ

there were 270 consecutive bases missing in cDNA sequence of the *NCED1* from HWWZSTJ (Fig. 6). Phylogenetic analysis showed that *CLH*, *DVR*, *PSY* and *NCED1* belonged to the same cluster, and their homology in comparison with similar sequences derived from other species is depicted in Figs. S13–S16. Results from sequence analyses suggested that deletion of 270 nucleotides in *NCED1* may be result in late-maturing characteristics of HWWZSTJ.

## DISCUSSION

Chlorophyll degradation, carotenoid biosynthesis and ABA metabolism play important roles in regulating citrus fruit maturation through a series of related genes or special signal network (*Zhang et al., 2014*). In this study, RNA-Seq technology was used to screen DEGs between a late-maturing mandarin mutant HWWZSTJ and its wild type WZSTJ during fruit maturation. DEGs between any two of the three libraries were significantly enriched in biological processes such as photosynthesis, phenylpropanoid biosynthesis, carotenoid biosynthesis, chlorophyll metabolism, ABA metabolism, starch and sucrose metabolism (*Table 3*). Thirteen maturing-related transcripts involved in carotenoid biosynthesis, chlorophyll degradation and ABA metabolism were selected for further analysis.

CLH is the key enzyme catalyzing the first step in the chlorophyll degradation. It can catalyze the hydrolysis of ester bond to yield chlorophyllide and phytol in the chlorophyll breakdown pathway (*Jacob-Wilk et al., 1999; Tsuchiya & Takamiya, 1999*). *Jacob-Wilk et al. (1999)* isolated a CLH encoding an active chlorophyllase enzyme and verified the role of CLH in chlorophyll dephytylation by *in vitro* recombinant enzyme assays. Expression level of *CLH* in Valencia orange peel was low and constitutive and did not significantly increase during fruit development and ripening (*Jacob-Wilk et al., 1999*). In the present study, a *CLH* was obtained from the transcriptome dataset. No difference was detected in the amino acid sequences of *CLH* between HWWZSTJ and WZSTJ. Expression levels of *CLH* were increasing prior to citrus fruit maturing, decreasing thereafter in both WZSTJ and HWWZSTJ. The highest expression level of *CLH* was detected on the 295<sup>th</sup> DAF in HWWZSTJ, which was 20 d later than that of WZSTJ (*Fig. 3*). Similar results were also observed in peels of the late-maturing mutant from Fengjie72-1 navel orange (*Liu et al., 2006*) and Tardivo clementine mandarin (*Distefano et al., 2009*). Those results suggested that *CLH* may balance between chlorophyll synthesis and its breakdown (*Jacob-Wilk et al., 1999*).

Citrus is a complex source of carotenoids with the largest number of carotenoids (*Kato et al., 2004*). Carotenoid contents and compositions are main factors that affect peel color of most citrus fruits (*Tadeo et al., 2008*). PSY is a regulatory enzyme in carotenoid biosynthesis (*Welsch et al., 2000*). PSY is present at low expression level in unripe (green) melon fruit, reaches its highest levels when the fruit turns from green to orange and persists at lower levels during later ripening stages (*Karvouni et al., 1995*). *Liu et al. (2006)* studied the mechanism underlying the difference between Fengwan (a late-maturing mutant) navel orange and its original cultivar (Fengjie72-1). The highest expression levels of some carotenoid biosynthetic enzymes in the peels of the late-maturing mutant occurred 30 d later than that of the original cultivar (*Liu et al., 2006*). In this work, PSY showed a trend from rise to decline at all fruit maturation stages of the late-maturing mutant HWWZSTJ and its original line WZSTJ. The expression levels of PSY3, PSY5, PSY6 and PSY7 in HWWZSTJ were lower than that in WZSTJ. These results demonstrated that the mutation in HWWZSTJ influenced the transcriptional activation of PSY.

ABA can be considered as a ripening regulator during fruit maturation and ripening. NCED, a key enzyme involved in ABA biosynthesis, plays an important role in fruit

ripening of avocado (*Persea americana*) (Chernys & Zeevaart, 2007), orange (*Citrus sinensis*) (Rodrigo, Alquezar & Zacarías, 2006), tomato (*Solanum lycopersicum*) (Nitsch et al., 2009; Zhang, Yuan & Leng, 2009), grape (*Vitis vinifera*) and peach (*Prunus persica*) (Zhang et al., 2009). The *NCED1* were expressed only at the onset stage of ripening in peach and grape, when ABA content became high (Zhang et al., 2009). Zhang et al. (2014) studied the mechanism of a spontaneous late-maturing mutant of 'Jincheng' sweet orange and its wild type through the comparative analysis. The highest expression of *CsNCED1* was at 215 DAA in WT. In our study, expression levels of *NCED1* increased prior to fruit maturing and decreased significantly thereafter in both HWWZSTJ and WZSTJ. The highest expression level of *NCED1* was detected on the 305<sup>th</sup> DAF of WT (WZSTJ). Our results were consistent with previous findings that *NCED1* plays the most important role in the ABA biosynthesis pathway during the fruit maturing process (Zhang et al., 2014). Deletion of nucleotides could cause a shift of the reading frame and truncated protein, which can result in natural mutants. Compared with the cDNA sequence of *NCED1* from WZSTJ, there were 270 consecutive bases missing in HWWZSTJ (Fig. 6). Those results suggested that *NCED1* might play an important role in late-maturing of HWWZSTJ. A high-efficient regeneration system for WZSTJ has been established (Wang et al., 2015) and further study on the role of *NCED1* in citrus is being carried out through genetic engineering.

## CONCLUSION

RNA-Seq technology was used to identify pigment-related genes from a late-maturing mandarin mutant HWWZSTJ and its original cultivar WZSTJ. Thirteen candidate transcripts related to chlorophyll metabolism, carotenoid biosynthesis and ABA metabolism were obtained. *NCED1*, a gene involved in ABA metabolism, is probably involved in the formation of late maturity of HWWZSTJ based on sequence and expression analyses. The present study opens up a new perspective to study the formation of late maturity in citrus fruit.

## ACKNOWLEDGEMENTS

We thank Peng Li, Zixing Ye and Jietang Zhao for help and support with field management and technical assistance.

## ADDITIONAL INFORMATION AND DECLARATIONS

### Funding

This work was supported by the Science and Technology Planning Project of Guangdong Province (2010B020305007), Key Laboratory of Innovation and Utilization for Germplasm Resources in Horticultural Crops in Southern China of Guangdong Higher Education Institutes, the South China Agricultural University (No. KBL11008). The funders had no role in study design, data collection and analysis, decision to publish, or preparation of the manuscript.

### Grant Disclosures

The following grant information was disclosed by the authors:

Science and Technology Planning Project of Guangdong Province: 2010B020305007.

Key Laboratory of Innovation and Utilization for Germplasm Resources in Horticultural Crops in Southern China of Guangdong Higher Education Institutes.

South China Agricultural University: KBL11008.

### Competing Interests

The authors declare there are no competing interests.

### Author Contributions

- Lu Wang performed the experiments, analyzed the data, contributed reagents/materials/analysis tools, wrote the paper, prepared figures and/or tables, reviewed drafts of the paper.
- Qingzhu Hua and Yuewen Ma performed the experiments, contributed reagents/materials/analysis tools, reviewed drafts of the paper.
- Guibing Hu analyzed the data, reviewed drafts of the paper.
- Yonghua Qin conceived and designed the experiments, analyzed the data, wrote the paper, prepared figures and/or tables, reviewed drafts of the paper.

### Data Availability

The following information was supplied regarding data availability:

The raw data has been supplied as [File S1](#).

### Supplemental Information

Supplemental information for this article can be found online at <http://dx.doi.org/10.7717/peerj.3343#supplemental-information>.

## REFERENCES

- Altschul S, Madden T, Schäffer AA, Zhang J, Zhang Z, Miller W, Lipman DJ. 1997. Gapped BLAST and PSI-BLAST, a new generation of protein database search programs. *Nucleic Acids Research* 25:3389–3402 DOI 10.1093/nar/25.17.3389.
- Bastías A, López-Climent M, Valcárcel M, Rosello S, Gómez-Cadenas A, Casaretto JA. 2011. Modulation of organic acids and sugar content in tomato fruits by an abscisic acid-regulated transcription factor. *Physiologia Plantarum* 141:215–226 DOI 10.1111/j.1399-3054.2010.01435.x.
- Chernys JT, Zeevaart JAD. 2007. Characterization of the 9-cis-epoxycarotenoid dioxygenase gene family and the regulation of abscisic acid biosynthesis in avocado. *Plant Physiology* 124:343–353 DOI 10.1104/pp.124.1.343.
- Deng YY, Li JQ, Wu SF, Zhu YP, Chen YW, He FC. 2006. Integrated nr database in protein annotation system and its localization. *Computer Engineering* 5:71–74.
- Distefano G, Casas G, Caruso M, Todaro A, Rapisarda P, La Malfa S, Gentile A, Tribulato E. 2009. Physiological and molecular analysis of the maturation process



- in fruits of clementine mandarin and one of its late-ripening mutants. *Journal of Agricultural and Food Chemistry* 57:7974–7982 DOI 10.1021/jf900710v.
- Food and Agricultural Organization of the United Nations** 2014. FAOSTAT. Available at [http://faostat.fao.org/site/567/DesktopDefault.aspx?PageID=\\$567#ancor](http://faostat.fao.org/site/567/DesktopDefault.aspx?PageID=$567#ancor).
- Ghosh S, Meli VS, Kumar A, Thakur A, Chakraborty N, Chakraborty S, Datta A.** 2011. The N-glycan processing enzymes  $\alpha$ -mannosidase and  $\beta$ -D-N-acetylhexosaminidase are involved in ripening-associated softening in the non-climacteric fruits of capsicum. *Journal of Experimental Botany* 62(2):571–582 DOI 10.1093/jxb/erq289.
- Harris MA, Clark J, Ireland A, Lomax J, Ashburner M, Foulger R, Eilbeck K, Lewis S, Marshall B, Mungall C, Richter J, Rubin GM, Blake JA, Bult C, Dolan M, Drabkin H, Eppig JT, Hill DP, Ni L, Ringwald M, Balakrishnan R, Cherry JM, Christie KR, Costanzo MC, Dwight SS, Engel S, Fisk DG, Hirschman JE, Hong EL, Nash RS, Sethuraman A, Theesfeld CL, Botstein D, Dolinski K, Feierbach B, Berardini T, Mundodi S, Rhee SY, Apweiler R, Barrell D, Camon E, Dimmer E, Lee V, Chisholm R, Gaudet P, Kibbe W, Kishore R, Schwarz EM, Sternberg P, Gwinn M, Hannick L, Wortman J, Berriman M, Wood V, Cruz N, Tonellato P, Jaiswal P, Seigfried T, White R.** 2004. The Gene Ontology (GO) database and informatics resource. *Nucleic Acids Research* 32:258–261 DOI 10.1093/nar/gkh036.
- Jacob-Wilk D, Holland D, Goldschmidt EE, Riov J, Eyal Y.** 1999. Chlorophyll breakdown by chlorophyllase: isolation and functional expression of the *Chlase1* gene from ethylene-treated *Citrus* fruit and its regulation during development. *Plant Journal* 20:653–661 DOI 10.1046/j.1365-3113X.1999.00637.x.
- Jia HF, Chai YM, Li CJ, Lu D, Luo JJ, Qin L, Shen YY.** 2011. Abscisic acid plays an important role in the regulation of strawberry fruit ripening. *Plant Physiology* 157:188–199 DOI 10.1104/pp.111.177311.
- Kanehisa M, Goto S, Kawashima S, Okuno Y, Hattori M.** 2004. The KEGG resource for deciphering the genome. *Nucleic Acids Research* 32:277–280 DOI 10.1093/nar/gkh063.
- Karppinen K, Hirvela E, Nevala T, Sipari N, Suokas M, Jaakola L.** 2013. Changes in the abscisic acid levels and related gene expression during fruit development and ripening in bilberry (*Vaccinium myrtillus* L.). *Phytochemistry* 95:127–134 DOI 10.1016/j.phytochem.2013.06.023.
- Karvouni Z, John I, Taylor J, Watson CF, Turner AJ, Grierson D.** 1995. Isolation and characterisation of a melon cDNA clone encoding phytoene synthase. *Plant Molecular Biology* 27:1153–1162 DOI 10.1007/BF00020888.
- Kato M, Ikoma Y, Matsumoto H, Kuniga T, Nakajima N, Yoshida T, Yano M.** 2004. Accumulation of carotenoids and expression of carotenoid biosynthetic genes during maturation in citrus fruit. *Plant Physiology* 134:824–837 DOI 10.1104/pp.103.031104.
- Koyama K, Sadamatsu K, Goto-Yamamoto N.** 2010. Abscisic acid stimulated ripening and gene expression in berry skins of the *Cabernet Sauvignon* grape. *Functional & Integrative Genomics* 10:367–381 DOI 10.1007/s10142-009-0145-8.

- Kumar R, Khurana A, Sharma AK. 2014.** Role of plant hormones and their interplay in development and ripening of fleshy fruits. *Journal of Experimental Botany* 65:4561–4575 DOI 10.1093/jxb/eru277.
- Leng P, Zhang GL, Li XX, Wang LH, Zheng ZM. 2009.** Cloning of 9-cis-epoxycarotenoid dioxygenase (NCED) gene encoding a key enzyme during abscisic acid (ABA) biosynthesis and ABA regulated ethylene production in detached young persimmon calyx. *Chinese Science Bulletin* 54:2830–2838 DOI 10.1007/s11434-009-0486-7.
- Liotenberg S, North H, Marion-Poll A. 1999.** Molecular biology and regulation of abscisic acid biosynthesis in plants. *Plant Physiology and Biochemistry* 37:341–350 DOI 10.1016/S0981-9428(99)80040-0.
- Liu Y, Tang P, Tao N, Xu Q, Peng SA, Deng XX, Xiang KS, Huang RH. 2006.** Fruit coloration difference between Fengwan, a late-maturing mutant and its original cultivar Fengjie 72-1 of Navel Orange (*Citrus sinensis* Osbeck). *Zhiwu Shengli Yu Fenzi Shengwuxue Xuebao* 32:31–36.
- Livak KJ, Schmittgen TD. 2011.** Analysis of relative gene expression data using real-time quantitative PCR and the  $2^{-\Delta\Delta CT}$  method. *Methods* 25:402–408 DOI 10.1006/meth.2001.1262.
- Luchi S, Kobayashi M, Taji T, Naramoto M, Seki M, Kato T, Tabata S, Kakubari Y, Yamaguchi-Shinozaki K, Shinozaki K. 2001.** Regulation of drought tolerance by gene manipulation of 9-cis-epoxycarotenoid dioxygenase, a key enzyme in abscisic acid biosynthesis in *Arabidopsis*. *Plant Journal* 27:325–333 DOI 10.1046/j.1365-313x.2001.01096.x.
- Nicolas P, Lecourieux D, Kappel C, Cluzet S, Cramer G, Delrot S, Lecourieux F. 2014.** The bZIP transcription factor *VvABF2* is an important transcriptional regulator of ABA-dependent grape berry ripening processes. *Plant Physiology* 164:365–383 DOI 10.1104/pp.113.231977.
- Nitsch L, Oplaat C, Feron R, Ma Q, Wolters-Arts M, Hedden P, Mariani C, Vriezen W.H. 2009.** Abscisic acid levels in tomato ovaries are regulated by *LeNCED1* and *SlCYP707A1*. *Planta* 229:1335–1346 DOI 10.1007/s00425-009-0913-7.
- Qin YH, Li GY, Wang L, Jaime A, Ye ZX, Feng QR, Hu GB. 2015.** A comparative study between a late-ripening mutant of citrus and its original line in fruit coloration, sugar and acid metabolism at all fruit maturation stage. *Fruits* 70:5–11 DOI 10.1051/fruits/2014037.
- Qin YH, Ye ZX, Hu GB, Li GY, Chen JZ, Lin SQ. 2013.** ‘Huawan Wuzi Shatangju’, a late-maturing mandarin cultivar. *Acta Horticulturae Sinica* 40:1411–1412.
- Rodrigo MJ, Alquezar B, Zacarías L. 2006.** Cloning and characterization of two 9-cis-epoxycarotenoid dioxygenase genes, differentially regulated during fruit maturation and under stress conditions, from orange (*Citrus sinensis* L. Osbeck). *Journal of Experimental Botany* 57:633–643 DOI 10.1093/jxb/erj048.
- Romero P, Lafuente MT, Rodrigo MJ. 2012.** The *Citrus* ABA signalosome, identification and transcriptional regulation during sweet orange fruit ripening and leaf dehydration. *Journal of Experimental Botany* 63:4931–4945 DOI 10.1093/jxb/ers168.

- Soto A, Ruiz K, Ravaglia D, Costa G, Torrigiani P. 2013.** ABA may promote or delay peach fruit ripening through modulation of ripening and hormone-related gene expression depending on the developmental stage. *Plant Physiology and Biochemistry* 64:11–24 DOI 10.1016/j.plaphy.2012.12.011.
- Sun L, Sun YF, Zhang M, Wang L, Ren J, Cui M, Wang YP, Ji K, Li P, Li Q, Chen P, Dai SJ, Duan CR, Wu Y, Leng P. 2012.** Suppression of 9-cis-Epoxycarotenoid dioxygenase, which encodes a key enzyme in abscisic acid biosynthesis, alters fruit texture in transgenic tomato. *Plant Physiology* 158:283–298 DOI 10.1104/pp.111.186866.
- Sun L, Wang YP, Chen P, Ren J, Ji K, Li Q, Li P, Dai SJ, Leng P. 2011.** Transcriptional regulation of *SLPYL*, *SLPP2C*, and *SlSnRK2* gene families encoding ABA signal core components during tomato fruit development and drought stress. *Journal of Experimental Botany* 62:5659–5669 DOI 10.1093/jxb/err252.
- Sun L, Zhang M, Ren J, Qi J, Zhang G, Leng P. 2010.** Reciprocity between abscisic acid and ethylene at the onset of berry ripening and after harvest. *BMC Plant Biology* 10:257–268 DOI 10.1186/1471-2229-10-257.
- Tadeo FR, Cercos M, Colmenero-Flores JM, Iglesias DJ, Naranjo MA, Rios G, Carrera E, Ruiz-Rivero O, Lliso I, Morillon R, Ollitrault P, Talon M. 2008.** Molecular physiology of development and quality of citrus. *Advances in Botanical Research* 47:147–223 DOI 10.1016/S0065-2296(08)00004-9.
- Tatusov R, Galperin M, Natale D, Koonin EV. 2000.** The COG database, a tool for genome-scale analysis of protein functions and evolution. *Nucleic Acids Research* 28:33–36 DOI 10.1093/nar/28.1.33.
- Trapnell C, Pachter L, Salzberg SL. 2009.** TopHat: discovering splice junctions with RNA-Seq. *Bioinformatics* 25:1105–1111 DOI 10.1093/bioinformatics/btp120.
- Tsuchiya T, Takamiya KI. 1999.** Cloning of chlorophyllase, the key enzyme in chlorophyll degradation, finding of a lipase motif and the induction by methyl jasmonate. *Proceedings of the National Academy of Sciences of the United States of America* 96:15362–15367 DOI 10.1073/pnas.96.26.15362.
- Wang J, Chen DJ, Lei Y, Chang JW, Hao BH, Xing F, Li S, Xu Q, Deng XX, Chen LL. 2014.** *Citrus sinensis* annotation project (CAP): a comprehensive database for sweet orange genome. *PLOS ONE* 9:e87723 DOI 10.1371/journal.pone.0087723.
- Wang L, Li P, Su CL, Ma YW, Yan L, Hu GB, Qin YH. 2015.** Establishment of a high-efficient regeneration system for Wuzhishatangju. *South China Fruits* 44:48–51.
- Wang YP, Wang Y, Ji K, Dai SJ, Hu Y, Sun L, Li Q, Chen P, Sun YF, Duan CR, Wu Y, Luo H, Zhang D, Guo YD, Leng P. 2013.** The role of abscisic acid in regulating cucumber fruit development and ripening and its transcriptional regulation. *Plant Physiology and Biochemistry* 64:70–79 DOI 10.1016/j.plaphy.2012.12.015.
- Wang XH, Yin W, Wu JX, Chai LJ, Yi HL. 2016.** Effects of exogenous abscisic acid on the expression of citrus fruit ripening-related genes and fruit ripenin. *Scientia Horticulturae* 201:175–183 DOI 10.1016/j.scienta.2015.12.024.
- Welsch R, Beyer P, Hugueney P, Kleinig H, Von Lintig J. 2000.** Regulation and activation of phytoene synthase, a key enzyme in carotenoid biosynthesis, during photomorphogenesis. *Planta* 211:846–854 DOI 10.1007/s004250000352.

- Xu Q, Chen LL, Ruan X, Chen D, Zhu A, Chen C, Bertrand D, Jiao WB, Hao BH, Lyon MP, Chen J, Gao S, Xing F, Lan H, Chang JW, Ge X, Lei Y, Hu Q, Miao Y, Wang L, Xiao S, Biswas MK, Zeng W, Guo F, Cao H, Yang X, Xu XW, Cheng YJ, Xu J, Liu JH, Luo OJ, Tang Z, Guo WW, Kuang H, Zhang HY, Roose ML, Nagarajan N, Deng XX, Ruan Y. 2013.** The draft genome of sweet orange (*Citrus sinensis*). *Nature Genetics* **45**:59–66 DOI [10.1038/ng.2472](https://doi.org/10.1038/ng.2472).
- Zhang M, Leng P, Zhang G, Li X. 2009.** Cloning and functional analysis of 9-cis-epoxycarotenoid dioxygenase (NCED) genes encoding a key enzyme during abscisic acid biosynthesis from peach and grape fruits. *Journal of Plant Physiology* **166**:1241–1252 DOI [10.1016/j.jplph.2009.01.013](https://doi.org/10.1016/j.jplph.2009.01.013).
- Zhang YJ, Wang XJ, Wu JX, Chen SY, Chen H, Chai LJ, Yi HL. 2014.** Comparative transcriptome analyses between a spontaneous late-ripening sweet orange mutant and its wild type suggest the functions of ABA, sucrose and JA during citrus fruit ripening. *PLOS ONE* **9**:e116056 DOI [10.1371/journal.pone.0116056](https://doi.org/10.1371/journal.pone.0116056).
- Zhang M, Yuan B, Leng P. 2009.** The role of ABA in triggering ethylene biosynthesis and ripening of tomato fruit. *Journal of Experimental Botany* **60**:1579–1588 DOI [10.1093/jxb/erp026](https://doi.org/10.1093/jxb/erp026).